Biophysical Chemistry, 34 (1989) 169–175
Elsevier

BIOCHE 01384

Cooperative coupling in allosteric systems

George H. Czerlinski

Northwestern University, 301 E. Chicago Avenue, Chicago, IL 60611, U.S.A.

Received 21 November 1988
Revised manuscript received 27 February 1989
Accepted 19 June 1989

Binding cooperativity; Allosteric model; Cooperative coupling; Chemical relaxation

Allosterism of the Monod type applies only to systems with more than one binding site and two (noncooperative) states with intrinsic binding constants. Allosterism is then defined by an interconversion constant L_0 (>1) and a ratio of intrinsic binding constants, c (<1). The value of c determines whether weak or strong cooperativity among binding sites prevails. Cooperativity is weak, if $1 > c > 0.1$, and strong, when $c \leq 0.1$. Cooperativity is the stronger, the smaller c. Cooperativity may exist only between a restricted number of binding sites. The binding of Ca^{2+} to calmodulin shows this behavior under certain conditions. An (internal) indicator for binding may signal binding to both states or to only one. The results would be quite different with the extent of the difference determined by the extent of cooperativity (c in relation to the particular L_i near 1). The size of L_0 cannot be ignored in reference to the size of c. Effectors external to the ligand could alter L_0 to shift cooperative behavior. Effectors could also make L_0 too small or too large for any allosteric behavior to appear.

1. Introduction

When Kirschner et al. [1] looked at the chemical relaxation of the binding of NAD^+ to yeast D-glyceraldehyde-3-phosphate dehydrogenase, they could easily evaluate all parameters on the basis of the Monod model at 40°C and pH 8.5. The restriction in temperature and pH was given by the fact that the introductory equilibrium titration experiments showed slight sigmoidal characteristics only under these conditions. Actually, the difference between the two individual (intrinsic) dissociation constants was quite small: $c = K_R/K_T = 0.35$. They found $L_0 = [T_0]/[R_0] = 30.5$, giving $L_n = c^n L_0 = 0.45$ with $n = 4$. Their comparatively large value for c (meaning: weak cooperativity) allowed them to 'detect' the interconversion of states for several L_i ($= [T_i]/[R_i]$). However, they were not able to detect L_0 and L_1 directly because of the detection limit. This is indicated in their fig. 6c, where $1/\tau$ (the inverse slowest relaxation time) is already rather steep at the lowest concentrations of NAD^+ used.

High cooperativity is indicated by $c \leq 0.1$. In this case, only very few L_i are directly detectable by chemical relaxation. The limit in the detection is given by the relative size of the observed equilibrium concentration change for the slowest relaxation process (involving the interconversion); actually, the equilibrium signal change is the key parameter, which will be discussed briefly. Equilibrium signal changes were first considered by Czerlinski [2–4], and later with some modifications by Thusius [5]. They will be considered here in some detail to demonstrate the limitations in detection specifically for $c \leq 0.1$.

2. Basic considerations

To facilitate the discussion, the original scheme of Monod et al. [6] is shown in fig. 1 with the following changes. The arrows for ligand binding

Correspondence address: G.H. Czerlinski, Northwestern University, 301 E. Chicago Avenue, Chicago, IL 60611, U.S.A.

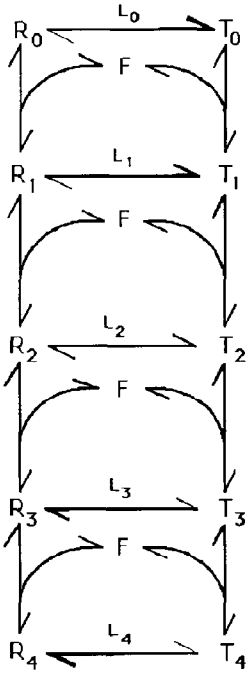

Fig. 1. Monod's model of allosteric interconversion for four binding sites of the ligand F, indicating by the thickness of the arrows the direction of the unimolecular interconversions and adjusted such that the concentrations of R_2 and T_2 are equal.

are arranged vertically with each participant in a reaction step having part of an arrow pointing to it. All isomeric interconversions are indicated by horizontal arrows. The thickness of the arrowheads of the double-ended arrows indicates the direction of the interconversion equilibria, set to equal unity for the 'middle' interconversion in fig. 1 and for the last interconversion in fig. 2 (with $n = 4$ being the total number of binding domains). Figs. 1 and 2 represent two specific cases, which will be discussed under various conditions.

If i is any number between 0 and n, the interconversion constants are defined by (brackets denote concentrations, subscripts designating the number of ligands bound)

$$L_i = [T_i]/[R_i] \text{ with } L_0 > 1 \qquad (1)$$

The intrinsic dissociation constants for the two states are K_R and K_T with their ratio given by

$$c = K_R/K_T < 1 \qquad (2)$$

Because of the cyclic character of the system ($i = 1, \ldots, n$)

$$L_i = cL_{i-1} \qquad (3)$$

The relation to unity in eqs. 1 and 2 is one of the basic definitions of the system with, in general, $L_0 \gg 1$.

The arrows in fig. 1 have been arranged such that $L_2 = 1$. The remaining L_i are then easily computed using the value of c and eq. 3. Strong cooperativity is indicated by $c \leq 0.1$. However, this condition makes the concentrations of R_0 compared to T_0 and of R_1 compared to T_1 'negligibly small' under most experimental conditions. After the interconversion ($L_2 = 1$) the relationships are reversed: the concentrations of T_4 compared to R_4 and T_3 compared to R_3 become negligibly small under most experimental conditions. Thus, the model of fig. 1 reduces to that of

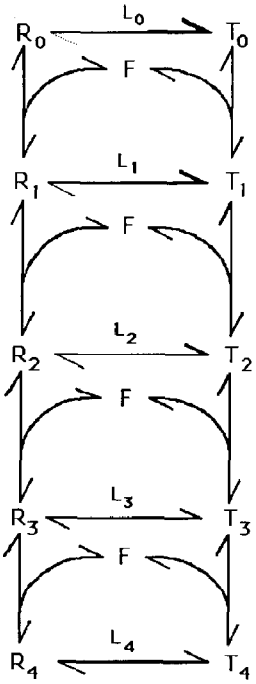

Fig. 2. Monod's model of allosteric interconversion for four binding sites of the ligand F, indicating by the thickness of the arrows the direction of the unimolecular interconversions and adjusted such that the concentrations of R_4 and T_4 are equal.

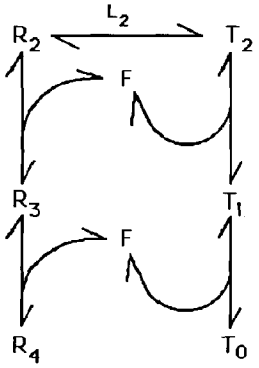

Fig. 3. The model of fig. 1 simplified under the condition that the ratio of intrinsic dissociation constants is sufficiently small, meaning: $c = K_R/K_T \leq 0.1$.

fig. 3. Fig. 3 may include the rate constants k_1 and k_2 with $L_2 = k_1/k_2$.

The arrows in fig. 2 are arranged such that $L_4 = 1$. The remaining L_i are then easily computed with the value of c and eq. 3. Now, condition $c \leq 0.1$ leads to the unusual result that the concentrations of R_0–R_3 are negligibly small compared to the corresponding T_i. Only $[R_4] = [T_4]$ at equilibrium (as $L_4 = 1$). One obtains the reaction scheme depicted in fig. 4. Chemical relaxation times for the sequential reactions of figs. 3 and 4 may easily be derived [4].

The condition $c \leq 0.1$ allows further simplifications for an initial estimate of parameter values. At very low concentrations, only the conversion from T_0 to T_1 needs to be considered. If the equilibrium constant for this dissociation process, $K_{1,T}$, is quite small (as for the binding of Ca^{2+} to calmodulin), the simplifying experimental condition of 'buffering' (meaning ligand $[F]^0 \gg$ total concentration of the allosteric protein) cannot be implemented. One therefore implements $[F]^0 = [T_0] + [T_1]$. The optimum for detection of chemical relaxation then lies at $[T_0] = [T_1] = K_{1,T}$, and thus $[F]^0 = 2K_{1,T}$.

Depending upon the indicating parameter, one either implements $[F]^0 = [T_0] + [T_1] + [T_2] + [R_2]$ or K_2, $[F]^0 \gg [T_0] + [T_1] + [T_2] + [R_2]$ for the study of the second dissociation process of the system of fig. 3. The same choices apply for the system of fig. 4, except that $[R_2] = 0$ in both relations ($[T_0]$ may also be negligible under most conditions).

Similar relations apply for the study of the third and fourth dissociation processes, except that the condition of equality of $[F]^0$ with the concentrations of the ligand receptors is less likely. Thus, for the system of fig. 3 one observes K_3, $[F]^0 \gg [T_2] + [R_2] + [R_3]$ and K_4, $[F]^0 \gg [R_3] + [R_4]$. On the other hand, for the system of fig. 4 one observes K_3, $[F]^0 \gg [T_2] + [T_3]$ and K_4, $[F]^0 \gg [T_3] + [T_4] + [R_4]$.

Figs. 3 and 4 represent idealized systems. Many other systems are possible, leading to changes in the relationships between $[F]^0$ and the concentrations of ligand receptors.

Strong cooperativity was defined by $c \leq 0.1$. In contrast, weak cooperativity may be defined by $1 > c > 0.1$. The above simplifications are not applicable for weak cooperativity and the equations of Kirschner et al. [1] need to be applied. How-

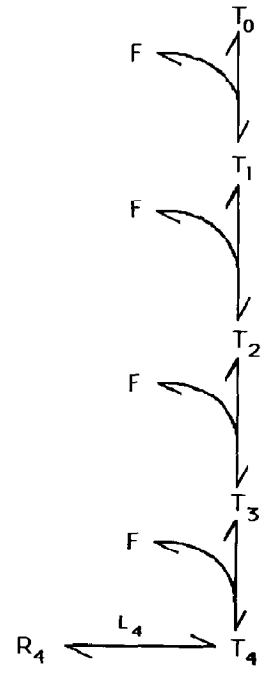

Fig. 4. The model of fig. 2 simplified under the condition that the ratio of intrinsic dissociation constants is sufficiently small, meaning: $c = K_R/K_T \leq 0.1$.

ever, the size of the concentration range that can be covered for detection of the slow relaxation process (identified with structural rearrangement between the R- and T-states) depends much on the actual value of c (and also upon the L_i, which is near 1). The larger the value of c, the greater is the number of interconversions between R- and T-states that are experimentally accessible. However, distinction between individual interconversions becomes difficult when c exceeds 0.5 (owing to excessive overlap).

Equilibrium signal changes for the detection of isomerizations are greatest when the two isomers (here R_i and T_i) are present at the same concentrations (most common, when isomers are not drastically different in their indicative properties (such as extinction coefficients)); in the case of isomers being very different in indicative properties, the isomer with the more pronounced indication (such as a relatively large extinction coefficient) should be present at lower concentration (see also ref. 4). For purposes of detectability, one

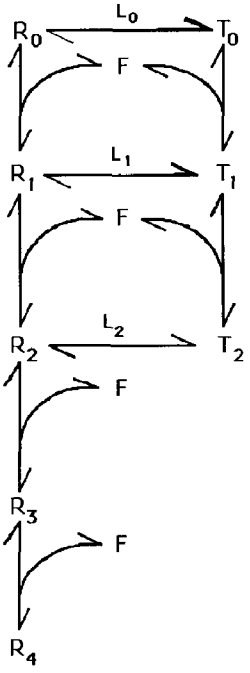

Fig. 5. Partial Monod model for a four-site protein with only the first two sites interacting; a hybrid model (may be derived from the data of Haiech et al. [7], table 1).

should then observe $0.1 \leq [R_i]/[T_i] \leq 10$. If c is very small ($c < 0.01$), this range of detectability for the isomerization may never be reached (namely, when $L_i > 10$ and $L_{i+1} < 0.1$). One would then find a large difference between K_i and K_{i+1} as $K_i = K_{i,T}$ and $K_{i+1} = K_{i+1,R}$ (with T and R referring to the prevailing states).

One could also consider a hybrid model of the type presented in fig. 5. Such a hybrid model seems to be particularly suited for calmodulin (Czerlinski, manuscript in preparation). In general, K_3 and K_4 in fig. 5 are not related to any intrinsic dissociation constant.

An allosteric interconversion model with $n = 2$ requires more parameters than the Adair model: The latter requires only two (K_1 and K_2), the former requires three (L_0, c, K_R). The allosteric model should therefore only be promoted, if strong indication for the interconversion is available.

Allosterism is undetectable for $L_n > 10$. There has to be some $L_i \approx 1$ (except for $i = 0$, as $L_0 > 1$ is a requirement). If $L_1 = 1$, little allosterism will be detectable at high [F], where only one state is present, even for weak cooperativity.

3. Specific applications

The 'hybrid' system of fig. 5 may readily be described in a quantitative manner; it is derived from specific data reported by Haiech et al. [7] on calmodulin. One may begin with expressing the total concentration of calmodulin, $[CAM]^0$, by the concentration of the individual components (eight terms).

To solve the system, two more equations are needed: The equation relating $K_{i,R}$ and the intrinsic constant K_R [6]:

$$K_{i,R} = \frac{[R_{i-1}][F]}{[R_i]} = \frac{i}{n-(i-1)} K_R, \tag{4}$$

and $K_{i,T}$ and intrinsic constant K_T:

$$K_{i,T} = \frac{[T_{i-1}][F]}{[T_i]} = \frac{i}{n-(i-1)} K_T. \tag{5}$$

One may then bracket $[R_0]$ out, and use eqs. 1, 2, 4 and 5 (in generalized form) with $n = 2$. The

dissociation constants K_3 and K_4 cannot be further expressed. One then obtains ($[CAM]^0$ = total concentration of calmodulin)

$$[R_0] = [CAM]^0/b \tag{6}$$

with

$$b = (1 + [F]/K_R)^2 + L_0(1 + c[F]/K_R)^2 + ([F]/K_R)^2([F]/K_3(1 + [F]/K_4))$$

If [F], the concentration of free allosteric effector (Ca^{2+} for calmodulin), is determined independently, b and thus $[R_0]$ may be computed. It is then easy to determine all the concentrations.

With $[R_0]$ known, all other concentrations of the components of calmodulin may be computed with eqs. 1, 4 and 5 (in generalized form). One may then formulate the ratios

$$Y_R = [\text{all R-forms with one or more Ca bound}]/[CAM]^0 \tag{7}$$

$$Y_T = [\text{all T-forms with one or more Ca bound}]/[CAM]^0 \tag{8}$$

These ratios are also readily computed (see ref. 4) for the hybrid system of fig. 5 (containing terms

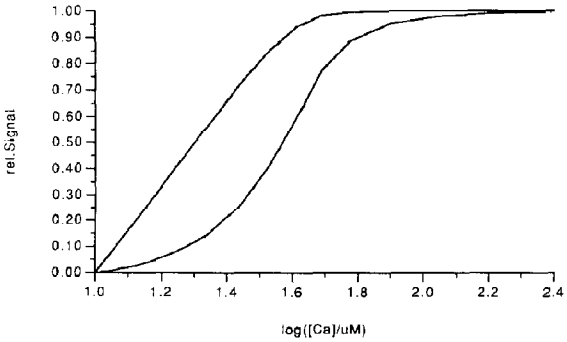

Fig. 6. Eq. 7 plotted as lower curve and eq. 9 as upper curve with $[CAM]^0 = 10$ μM. The abscissa gives the logarithm of the total concentration of calcium (in μM, relative to 1 μM). The following parameter values were used: $L_0 = 100$, $c = 0.1$, $K_R = 1$ μM and $n = 2$ (from model of fig. 5), $K_3 = 8$ μM, $K_4 = 32$ μM.

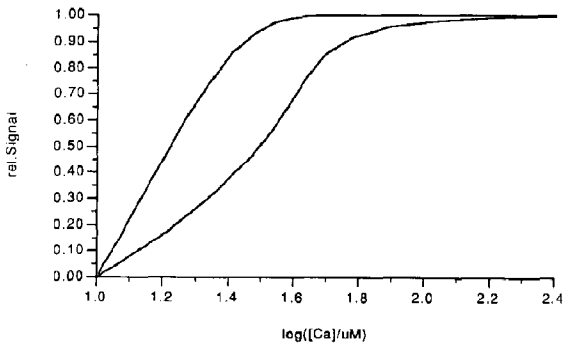

Fig. 7. Eq. 7 plotted as lower curve and eq. 9 as upper curve with $[CAM]^0 = 10$ μM. The abscissa gives the logarithm of the total concentration of calcium (in μM, relative to 1 μM). The following parameter values were used: $L_0 = 4$, $c = 0.5$, $K_R = 1$ μM and $n = 2$ (from model of fig. 5), $K_3 = 8$ μM, $K_4 = 32$ μM.

like those in b below eq. 6). One may also express the sum:

$$Y = Y_R + Y_T \tag{9}$$

Figs. 6 and 7 show graphs of Y_R (lower curve) and Y (upper curve) for a specific set of parameter values given in the figure legends. It should be pointed out that the logarithm of the concentration of Ca in μM (relative to 1 μM) is given on the abscissa. The difference between the two curves indicates that substantial amounts of T_1 and T_2 are present at lower concentrations of Ca. The upper curve reaches its saturation level at $[Ca]^0 = 3[CAM]^0$ for fig. 7, being slightly higher for fig. 6. While cooperativity is strongly indicated in fig. 6, it is weak in fig. 7. In fact, the cooperativity is so weak ($c = 0.5$) that one may not observe any indication of allosteric behavior in ordinary titrations (observing only Y). One needs R-specific indicators to discern the difference shown in fig. 7. Tryptophan, suitably incorporated into calmodulin by site-directed mutagenesis, could be such an indicator (Czerlinski, manuscript in preparation).

4. Discussion

The condition $c \leq 0.1$ allows one to express cyclic allosteric systems in terms of linear reaction sequences (figs. 3 and 4, respectively), leading to

simplified expressions for the chemical relaxation times of the system. However, cycles cannot be omitted if $L_i \cdot L_{i-1} \approx 1$ and $c \approx 0.1$ (e.g., $L_i = 0.33$, $L_{i-1} = 3.3$). As far as chemical relaxation is concerned, it is assumed that the slowest relaxation time is associated with the allosteric interconversion. This assumption may not always be fulfilled (which would not affect the equilibrium considerations).

The extent of cooperativity is indicated by the value of c: The smaller the value of c, the higher is the cooperativity. However, the concentration of ligand F at which this cooperativity becomes most pronounced, depends upon the size of L_0, connected to any L_i by eq. 3. When L_i is near unity, switch-over from the T-state to the R-state takes place.

Allosteric effectors may alter the magnitude of L_0. If L_0 is increased by an effector and c remains constant, switch-over from the T- to R-state occurs at higher values of i than without effector. Alternatively, if L_0 is decreased by an effector and c remains constant, switch-over from the T- to R-state takes place at lower values of i than in the absence of an effector. An effector abolishes allosterism (with c constant) when either $L_0 < 1$ or $c^n L_0 \geq 10$. In the former case, only R-states are present, and in the latter, only T-states, at any $[F]^0$.

The effect of different values of L_0 and c on the shape of curves for the hybrid model of fig. 5 is demonstrated in figs. 6 and 7. In both cases Y_R and Y have been plotted. Experimental distinction is possible only if binding of F to R differs from that to T and this difference shows up in the indicating parameter (offered by fluorescence).

It should be mentioned that cooperativity derived from the conditions of eqs. 1 and 2 is not always associated with an isomerization model (of Monod et al. [6]). The polymerization model may also be present [8]. The polymerization model can be easily distinguished from the isomerization model, as the former is dependent upon protein (enzyme) concentration, whereas the latter is not. Furthermore, kinetic detection of the (unimolecular) isomerization rate constants would prove the validity of an isomerization model.

All the above kinetic considerations implied that the time constants for the allosteric interconversions are much slower than those for the bimolecular associations. If they are not much slower, more complex equations apply (see ref. 4). If, on the other hand, the interconversions are much faster than the bimolecular steps, different considerations apply, given in the appendix.

Appendix

One special case was not considered in the above derivations: The unimolecular interconversions are much faster than the bimolecular association steps. In these cases, one could still obtain information from consecutive fast relaxation times, if these time constants are not too close together.

One readily derives (see eq. (2-53) of ref. 4 with $\bar{c}_1 = [T_i]$ and thus $K_{2,1} = L_i$):

$$\frac{\Delta[R_i]}{[R_i] + [T_i]} = \frac{L_i}{(1 + L_i)^2} \frac{\Delta L_i}{L_i} \tag{A1}$$

$\Delta L_i / L_i$ is directly related to the enthalpy change for this reaction step and is assumed to be 0.1 for convenience of evaluation. $\Delta[R_i]/([R_i] + [T_i])$ (which equals $\Delta[T_i]/([R_i] + [T_i])$) is the observed relative concentration change, which has a maximum at $L_i = 1$, decreasing on both sides (to 1/3 of maximum for $L_i = 10$ and 1/10). In other words, individual relaxation processes are experimentally accessible for $0.1 \leq L_i \leq 10$.

To consider chemical relaxation, the rate constants k_1 and k_2 are defined as being associated only with L_0 (in contrast to the definitions in the main text), meaning

$$L_0 = \frac{[T_0]}{[R_0]} = \frac{k_2}{k_1} \tag{A2}$$

As $L_i = L_0 c^i$, the factor c^i may be coupled with either k_2 or k_1 (the two cases of degeneracy [8]), or:

$$L_i = (k_2 c^i)/k_1 \tag{A3}$$

$$L_i = k_2 (c^i / k_1) \tag{A4}$$

These relationships have significance only for the

kinetic evaluations. In principle, one may distinguish the following $n+1$ fast relaxation times

$$\tau_i^{-1} = k_1 + k_2 c^i \quad \text{(A5)}$$

$$\tau_i^{-1} = k_1/c^i + k_2 \quad \text{(A6)}$$

The relaxation time τ_0 then refers to the relaxation time for the interconversion with L_0.

Although one may write $n+1$ expressions for relaxation times, only those for which $0.1 \leq L_i \leq 10$ may be detectable (see above). However, if these relaxation times are closer than factor 3 (this factor also depends upon the precision of the measurement and could become as small as 2), they can no longer be separated from each other. Separation requires $\tau_{i+1}/\tau_i > 3$ or $\tau_{i+1}/\tau_i < 1/3$, or $c < 0.33$. If $c < 0.1$, only two relaxation processes may be detectable. If $c \ll 0.1$, only one relaxation process may be detectable (or even none under unfavorable conditions). Thus, if the interconversions are fast, there may be only one concentration range of the effector within which a fast relaxation process is detectable. However, if L_0 and c are determined independently, the correlation of this interconversion to that involving L_0 and c can be established.

References

1 K. Kirschner, M. Eigen, R. Bittman and B. Voight, Proc. Natl. Acad. Sci. (U.S.A.) 56 (1966) 1661.
2 G. Czerlinski, J. Theor. Biol. 7 (1964) 435.
3 G. Czerlinski, J. Theor. Biol. 7 (1964) 463.
4 G. Czerlinski, Chemical relaxation. Introduction to stepwise perturbation (Dekker, New York, 1966).
5 D. Thusius, Biophys. Chem. 7 (1977) 87.
6 J. Monod, J. Wyman and J.-P. Changeux, J. Mol. Biol. 12 (1965) 88.
7 J. Haiech, C.B. Klee and J.G. Demaille, Biochemistry 20 (1981) 3890.
8 G. Czerlinski, Curr. Mod. Biol. 2 (1968) 219.